Are all Osteocytes Equal? Multiscale Modelling of Cortical Bone to Characterise the Mechanical Stimulation of Osteocytes

T.J. Vaughan, S.W, Verbruggen, L.M. McNamara*

Biomechanics Research Cluster (BMEC), National Centre for Biomedical Engineering Sciences (NCBES) and the Department of Mechanical and Biomedical Engineering, National University of Ireland, Galway.

Address for correspondence:
Dr. Laoise M. McNamara
Department of Mechanical and Biomedical Engineering
National University of Ireland Galway
Galway,
Ireland
Phone: (353) 91-492251
Fax: (353) 91-563991
Email: Laoise.McNamara@nuigalway.ie

Keywords of the paper: multiscale modelling, mechanotransduction, osteocyte, finite element analysis

Abstract

Bone continuously adapts its internal structure to accommodate the functional demands of its mechanical environment.This process is orchestrated by a network of mechanosensitive osteocytes that respond to external mechanical signals and recruit osteoblasts and osteoclasts to alter bone mass to meet loading demands. Due to the irregular hierarchical microarchitecture of bone tissue, the precise mechanical stimuli experienced by osteocytes located in different regions of the tissue is not well understood. The objectives of this study are to develop a progressive localisation framework that predicts how tissue level strains in cortical bone are related to the cellular level and characterise the local stimulus experienced by osteocytes distributed throughout the tissue structure. Our models predict that an inhomogeneous microstructural strain field contributes to osteocytes receiving a vastly different stimulus at the cellular level, depending on their location within the microstructure. In particular, osteocytes located directly adjacent to micro-pores experienced strain amplifications in their processes of up to nine times the applied global strain. Furthermore, it was found that the principal orientation of lamellar regions was found to contribute significantly to the magnitude of the stimulus being received at the cellular level. These findings indicate that osteocytes are not equal in terms of the mechanical stimulus being received and we propose that only a subset of osteocytes may be sufficiently stimulated to function as mechanoreceptors.

1.0 Introduction

Bone is an adaptive material whose structure and composition change to accommodate the demands of its mechanical environment. Physiological loading of the skeletal system through weight-bearing exercise activates the remodelling process that maintains or increases bone density, while disuse and immobilisation cause bone resorption and a loss in overall bone mass. It is hypothesised that this remodelling process is regulated at a cellular level through a network of mechanosensitive osteocytes, which monitor the mechanical environment and recruit osteoblasts and osteoclasts to alter bone mass to meet the loading demands [1-3]. It is believed that the mechanical environment is monitored by mechanoreceptors on the cell body and processes, such as integrins [4-6], gap junctions [7, 8] and primary cilia [9-11]. Mechanotransduction theories have proposed that osteocytes respond to mechanical signals caused by either direct stimulation of the cell body, as a result of mechanical strain of the extracellular tissue [12-17], or indirect stimulation of the cell body resulting from fluid flow through the lacunar-canalicular system [18-22]. These studies have been largely based on idealised computational or analytical studies of individual osteocytes [17-20]. However, osteocytes reside in a complex environment, which is characterised by a heterogeneous microstructural architecture, and no previous study has been able to understand the role of this complex microarchitecture on individual osteocytes.

Bone tissue is an intricate composite of organic proteins and mineral crystals that are hierarchically organised at multiple scales to form a highly optimised structure. At the microstructural level, cortical bone is arranged into osteons, which consist of concentric arrangements of lamellar bone intersected by vascular channels (Haversian and Volkmann Canals), whose function is to provide blood and nutrients to different regions of the tissue (Figure 1). At the sub-microstructural level, osteocytes are distributed throughout osteons and reside within lacunar and canalicular cavities, extending cell processes to other cells to form a connective network (Figure 1). An organic matrix surrounds the osteocyte within the

pericellular space and anchors the cell to the surrounding extracellular matrix [23]. This matrix is saturated with interstitial fluid, whose flow is driven by strain of the extracellular matrix causing shear stress to be imparted along the cell membrane. While loading patterns at the organ and tissue level have been predicted by high resolution finite element modelling techniques [24, 25], the mechanical stimulus being received at the cellular level is not well understood. Analytical studies have predicted the stimulus along idealised cell processes and proposed that strain amplification occurs in the extracellular matrix surrounding the cell body and processes [6, 18, 23, 26]. An experimental study characterised the strain field on an exposed plane using optical microscopy and found that peak strains in the vicinity of osteocyte lacunae could be an order of magnitude greater than tissue level strains measured in vivo [14, 15]. More detailed predictions of cellular deformation have been developed using computational finite element models that characterise the local mechanical environment of the osteocyte in vivo [15-17]. These models focus on local cellular strains and do not consider the effect of interstitial fluid flow on osteocyte deformation, despite the fact that many studies have proposed that fluid flow may be the primary mechanism through which an osteocyte senses it mechanical environment [18-22]. However, this approach seems justified as fluid-flow in the lacuna-canalicular system is largely a strain-driven phenomenon meaning that strain amplifications at the local cellular level would have as much an effect in stimulating the osteocyte through either strain based or fluid-flow based mechanotransduction. Recently, advanced high resolution confocal imaging has been used to develop geometrically accurate three-dimensional finite element models of the osteocyte environment [16]. These finite element models have shown that local strains in canalicular regions surrounding osteocyte cell processes are even higher than those predicted by idealised models, in some regions being eight times greater than the applied global strain [16]. However, these studies only focused on the individual cell level, and did not take into account the role of microstructural features, such as Haversian and Volkmann Canals, in dictating the strain environment of individual osteocytes.

Haversian and Volkmann canals contribute to the microstructural porosity of bone tissue and account for approximately 14% of the total volume of cortical bone [27] and have a significant effect on the organ level stiffness of bone tissue [28, 29]. These structures contribute to the development of inhomogeneous microstructural strain fields throughout the osteon under loading [28].Therefore, it is likely that osteocytes at different locations within the osteon may be receiving significantly different stimuli, with some being subject to further strain amplification effects depending on their location [28]. Furthermore, the surrounding extracellular tissue is arranged in lamellar packets that exhibit a preferential collagen fibre orientation leading to anisotropic behaviour, which could further affect the local stress state. However, to date no study has taken into account the irregular hierarchical microarchitecture of bone tissue when predicting the mechanical environment of osteocytes.

The objectives of this study are to (1) develop a progressive localisation framework that predicts how tissue level strains applied to cortical bone are related to the cellular level and (2) characterise the local stimulus experienced by osteocytes distributed throughout the tissue structure. This progressive localisation framework considers two levels of structural hierarchy within cortical bone tissue. The study incorporates important structural features at the microstructural level, such as micro-pores and discrete lamellar regions, and identifies the important contribution these features have in determining the local strains experienced by osteocytes in vivo. Using this progressive localisation technique, we investigate how cellular level strains may be related to applied loads at the tissue level and whether different osteocytes within cortical bone receive the same stimulus. The development of accurate models that capture loading patterns in the surrounding osteocyte environment is crucial to understand the cellular mechanisms associated with mechanotransduction in vivo.

2.0 Materials and Methods

2.1 Model Formulation

This model is formulated at two separate length scales. At the microstructural level, we develop a micromechanical model of an osteon embedded within interstitial tissue that includes structural details of discrete lamellar regions and Haversian and Volkmann Canals. Periodic boundary conditions are used to predict local microstructural stress/strain fields under macroscopically equivalent loads that represent typical tissue level strains observed in vivo. At the cellular scale, an idealised model of the osteocyte environment is coupled to the microstructural model of cortical bone through a submodelling technique, to relate tissue level loading to local cellular deformation. These models are described in further detail below.

(i) Osteon Model

At the microstructural level, it is assumed that the osteon is composed of eight discrete lamellar regions that are concentrically arranged around a Haversian Canal and are intersected by interconnecting Volkmann Canals in two transverse directions, as shown in Figure 2 (a). The overall osteon diameter is 200μm, the size of the Haversian canal is 80μm and the individual lamellar thickness is 7.5 μm, similar to our previous representation in [29]. The Volkmann Canals have a diameter of 50μm and we assume that the osteon is periodic in the longitudinal direction with a repeating unit of 200μm. The osteon is embedded in an outer region that represents a region of interstitial bone of dimensions 200μm × 210μm × 210μm. This micromechanical model was discretised using approximately 200,000 four-noded tetrahedral elements (C3D4) and was solved using the ABAQUS finite element code. Due to the orientation of collagen fibres within lamellar bone, we assume orthotropic behaviour of each lamellar region, where the principal collagen fibre orientation (θ_x) is defined with respect to its inclination from the longitudinal axis of the osteon, as shown in Figure 2 (a). This analysis considers two separate arrangements of lamellar bone tissue, a first case where the principal lamellar orientation of each successive lamellar region varies between +15°/-15° and a second

case where the principal lamellar orientation of each successive lamellar region varies between +45°/-45°. The interstitial region is assumed to behave as an orthotropic continuum, whose principal axis is aligned with the longitudinal direction (i.e. the 1-direction).

(ii) Cellular Submodel

The cellular submodel consists of an idealised representation of an osteocyte cell, surrounded by a pericellular matrix (PCM) that is embedded in the extracellular matrix (ECM), as shown by the sectioned view in Figure 2 (b). The osteocyte cell body was assumed to be an ellipsoid with minor and major axes equal to 7.5μm and 13.5μm, respectively, while the osteocyte cell processes were modelled as cylindrical extensions of diameter 0.44μm extending outward from the cell body [16]. The PCM surrounding the cell is assumed to be 0.75μm thick around the cell body and 0.08μm thick around the cell processes [5, 30, 31]. The osteocyte cell and surrounding PCM are embedded in an ECM region, which is a cuboid measuring 13μm × 13μm × 25μm. A continuous mesh is used to discretise all regions using approximately 500,000 tetrahedral elements (C3D4).

2.2 Boundary Conditions and Material Parameters

(i) Osteon Model

Periodic boundary conditions were applied to the osteonal model, enabling the prediction of microscopic quantities from applied macroscopic loading configurations and thus providing an effective means of relating tissue level and osteon level strains to one another. These boundary conditions consisted of a series of kinematic ties imposed on opposing faces of the unit cell and may be expressed in three-dimensions as,

$$\begin{aligned} \mathbf{u}(0, x_2, x_3) - \mathbf{u}(l, x_2, x_3) &= \mathbf{u}_1 \\ \mathbf{u}(x_1, 0, x_3) - \mathbf{u}(x_1, h, x_3) &= \mathbf{u}_2 \\ \mathbf{u}(x_1, x_2, 0) - \mathbf{u}(x_1, x_2, t) &= \mathbf{u}_3 \end{aligned} \tag{1}$$

where $\mathbf{u_1}$, $\mathbf{u_2}$ and $\mathbf{u_3}$ are the displacement vectors which relate the displacements on opposite faces of the unit cell shown in Figure 2 (a), while *l*, *h* and *t* correspond to the unit cell dimensions in the 1-, 2- and 3-directions, respectively.

A single loading case is considered whereby a compressive stress in the longitudinal direction of 20MPa was applied to the osteon model through a concentrated force applied at the master node. For the +15°/-15° lamellar arrangement, this load resulted in a global compressive strain of approximately 2,000με, which represents a typical tissue level load measured in vivo during physical exertion [32]. Each lamellar region was assigned orthotropic linear elastic behaviour, where the material parameters were chosen based on a homogenisation scheme developed in [29] that considers the fundamental constituents of hydroxyapatite crystals distributed within a collagen matrix, and the material parameters are listed in Table 1.

(ii) Cellular Submodel

At the cellular level, a submodelling technique was used to capture the local behaviour of the osteocyte and its surrounding environment. This technique is available in ABAQUS and uses a global-local approach to provide a detailed solution for structural details that require a highly resolved mesh. A node-based submodelling procedure is used whereby the boundary conditions applied to the submodel are interpolated from the nodal displacements in the global model. In this case, the solution for the osteon model is determined *a priori* and this may be used to impart deformation on the relevant boundaries of the cellular submodel, allowing an accurate prediction of global to local behaviour. In Figure 2 (b), the interpolated displacement field from the osteon model solution is applied to the nodes located on the external surfaces of the cellular submodel.

For the analysis, the osteocyte cell was assumed to behave as a compressible Neo-Hookean hyperelastic material, whose strain energy density function may be expressed by the following relation,

$$W = \frac{\mu_0}{2}\left(\bar{\lambda}_1^2 + \bar{\lambda}_2^2 + \bar{\lambda}_3^2 - 3\right) + \frac{\kappa_0}{2}\left(\lambda_1\lambda_2\lambda_3 - 1\right)^2 \qquad (2)$$

where W is the strain energy per unit reference volume, λ_i are the principal stretches, $\bar{\lambda}_i$ are the deviatoric principal stretches, while μ_0 and κ_0 are the initial shear and bulk moduli, respectively. The initial shear and bulk moduli may be related to elastic modulus (E) and Poisson's ratio (υ) using standard isotropic linear elastic relations. For the osteocyte, an elastic modulus of 4.47kPa and a Poisson's ratio of υ = 0.4 are assumed [33]. The surrounding PCM was assumed to behave as an isotropic linear elastic material with a Young's modulus of E = 40kPa and a Poisson's ratio of υ = 0.4 [34].

2.3 Distribution of cellular submodels

This analysis specifically investigates the mechanical stimulus being imparted to osteocytes in different regions of the cortical bone microstructure by systematically varying the location of the cellular submodel within the osteon global model. Osteocytes are distributed in a radial direction around the Haversian Canal in between individual lamellar regions, therefore this analysis considers cellular submodels in radial locations around the Haversian canal. These locations are identified in Figure 3 (a), where, due to symmetry, we only consider locations in one quadrant of the osteon. The location of these cellular submodels is also varied in the longitudinal direction and we consider the behaviour on three separate planes that are 25μm apart throughout the length of the osteon, as shown in Figure 3 (b)-(d). In total, 30 cellular submodels were analysed and the positions of these were varied throughout the osteon.

3.0 Results

3.1 Osteon Model

Figure 4(a) shows the distribution of minimum principal strain in a sectioned view of the osteon model with a +15°/-15° lamellar arrangement under a compressive stress of 20MPa applied in the longitudinal direction. This load resulted in a global compressive strain of approximately 2,000με and significant strain amplifications (by a factor of approximately 2.8) occur in the regions directly adjacent to the Volkmann Canals that traverse the osteon. The volume averaged distribution of minimum principal strain shown in Figure 4 (b) highlights the inhomogeneous strain field present under loading. Specifically, we predict that approximately 10% of volume of the osteon experiences strains of less than 1,000 με due to the strain relieving effects of the Volkmann Canals (See Figure 4 (a)). For a lamellar arrangement of +45°/-45°, a similar strain distribution is predicted in the osteon model (not shown) but the strain magnitudes are increased compared to the +15°/-15° model, as shown by the volume average distribution in Figure 4(b).

3.2 Cellular Submodels

Figure 5 shows a selection of the cellular submodels that were distributed throughout the osteon model that had a +15°/-15° lamellar arrangement. The osteocyte that experiences the greatest mechanical stimulus was located on Plane 1 and was directly adjacent to a Volkmann Canal relative to the loading direction in the osteon model, as shown in Figures 5a and d. This osteocyte was located between the two outermost lamellae and its centre axis was 13μm from the outer edge of the Volkmann Canal, as identified by Location A in Figure 3b. At this location, the microstructural strain field is significantly amplified (Figure 5a), leading to a minimum principal strain in the cellular model of 18,340με. This strain level occurred in the cell process that is in closest proximity to the Volkmann Canal and represents a strain amplification factor of 9 when compared to the applied tissue strain (2,000 με). The osteocyte that experiences the smallest mechanical stimulus was located on Plane 2 and was also adjacent

to a Volkmann Canal however was aligned with the loading direction (Figure 5b). This osteocyte was again located between the two outermost lamellae and its centre axis was directly in line with the centre axis of the Volkmann Canal below, as identified by Location B in Figure 3d. Here, the microstructural strain in the osteon model was less than 1,000 με (see Figure 5(a)), resulting in low strain magnitudes being transferred to the cellular model at this location.

Figure 6 shows the volume averaged distribution of minimum principal strain for the osteocytes that experience both the minimum and maximum mechanical stimulus, i.e. the same as those presented in Figure 5 (b) and (d), respectively. For a lamellar orientation of +15°/-15°, the osteocyte model that receives the greatest stimulus shows that approximately 70% of its volume experiences a compressive strain between 4,000-5,000με, while 0.3% of the cell experiences a stimulus of greater than 10,000με. From Figure 5 (d), these large strains occur in the process region of the cell. The predicted cellular strains when a lamellar orientation of +45°/-45° is considered are even higher than this, with approximately 70% of the cell volume experiencing a stimulus of greater than 5,000με. For the osteocyte model that receives the smallest stimulus, the majority of the cell volume experiences strains below 2,000με, which is below the global compressive strain, for both lamellar orientations are considered. Also shown in Figure 6 are the mean values of compressive strains from all 30 osteocytes that had lamellar orientations of +15°/-15°. It is predicted from these models that over 30% of the volume of all osteocytes experience strains between 3,000-4,000με, indicating that a large volume of all osteocytes experience a strain amplification of approximately 2. Finally, Figure 6(b) shows the volume averaged distribution of Minimum Principal strain for each plane considered, where, on average, the osteocytes located on Plane 1 experience a greater stimulus compared to those located on either Planes 2 or 3.

4.0 Discussion

A progressive localisation framework has been developed to predict how tissue level strains applied to cortical bone are related to the cellular level and has been applied to characterise the

nature of the stimulus experienced by osteocytes distributed throughout different regions of cortical bone tissue. The study incorporates important structural features at the microstructural level, such as Volkmann and Haversian canals and discrete lamellar regions, and identifies the important contribution these features have in determining the local strains experienced by osteocytes in vivo. The current study considers a network of osteocytes distributed throughout osteonal bone and predicts that different osteocytes may receive a vastly different mechanical stimulus, depending on their location in the cortical microstructure. In particular osteocytes that were directly adjacent to Volkmann Canals (e.g. Location X in Figure 5a) received a much greater stimulus than others due to strain amplification effects occurring at the microstructural levels. Interestingly, Volkmann canals also had strain relieving effects and for certain osteocytes that were directly aligned with Volkmann Canals and the direction of the applied load (e.g. Location Y in Figure 5a), the stimulus received was less than the applied tissue level loads. Furthermore, it was found that the lamellar orientation had a significant effect on the magnitude of cellular stimulus, with higher cellular strains present in cellular submodels when an orientation of +45°/-45° is considered, compared to a lamellar arrangement of +15°/-15°.

The current study may be subject to a number of potential limitations. Firstly the assumption of an idealised geometry for the cellular model may underestimate the strains experienced by osteocytes as a recent finite element study has shown that geometrically realistic cell models [16] are subject to higher strain amplifications when compared to idealised models. Furthermore, it was found in [16] that the presence of discrete attachments between the osteocyte and the ECM led to the presence of further strain concentrations. The inclusion of such features and realistic cell models would lead to the prediction of higher strain amplification values reported here. A recent study has proposed that osteocytes may alter their lacunar geometry to adapt to their local mechanical environment [35] and thus the strain signal being received [17], whereas this study assumes that all osteocytes have the same morphology. Our findings have shown that microstructural features greatly affect the stimulus received by a

given osteocyte, with a five-fold difference in strain magnitudes present between certain osteocytes in different locations within the microstructure. It has previously been shown that alteration of the local osteocyte environment has a much smaller effect on the strain signal being received, with significant changes in local tissue modulus and canalicular diameter leading to less than a 20% change in strain magnitudes experienced by the osteocyte [17]. Therefore, we chose not to vary the local lacunar morphology and our findings importantly highlight that features at the microstructural level have a much larger effect on the stimulus being received by the osteocyte. The prediction of cellular deformation is further complicated by the lack of experimental data regarding the mechanical behaviour of the osteocyte and surrounding environment. It should be noted that material parameters for the osteocyte were assumed from measurements of the peripheral elasticity of bone cells [33], while material parameters for the PCM refer to properties determined for a chondrocyte PCM [34]. Also, the current study characterises the mechanical stimulus at the cellular level in terms of mechanical strain experienced by the osteocyte and does not consider the effects of fluid shear stress imparted on the cell membrane due to interstitial fluid flow. While it has been hypothesised that cellular deformation resulting from fluid shear stress may be one of the primary mediators of mechanical stimuli in vivo [18-22], we assume that fluid flow within canalicular cavities is a strain-driven phenomenon. It should be noted however that recent studies [36, 37] have highlighted the fact that electrochemical phenomenona, in particular calcium gradients [36], could provide a significant contribution to shear stress imparted on the osteocyte cell membrane when compared with strain-driven fluid flow, however our model does not account for such effects.

At the microstructural level, the modelling approach assumes a geometrically periodic representation of cortical bone using an idealised osteon and as such cannot capture differences throughout the tissue structure (e.g. posterior and anterior locations of the bone). Furthermore, certain geometric aspects, such as differences in the vascular geometry, local porosity or

discrete damage events, could contribute to further inhomogeneity in the strain field. In particular, porosity may exist at the microstructural level due to the presence of resorption cavities, which have already been found to cause strain amplification effects under loading [38].

It has previously been shown that damage accumulation (in the form of lamellar micro-cracking, inter-lamellar debonding and cement line debonding) can lead to unloading of osteocyte lacunae [38]. It is interesting to note that the deformation characteristics predicted in our model due to micro-pores at the microstructural level are qualitatively comparable to those previously predicted surrounding bone damage [38]. For example, an increased stimulus is experienced by osteocytes directly adjacent to a micro-pore, which is similar to the deformation observed in lacunar regions directly adjacent to an inter-lamellar debonding site [38]. Furthermore, significant unloading of lacunar regions is observed once complete debonding had occurred at interface [38], which is similar to strain relieving effects observed around micro-pores in our study.

Several in vitro investigations have found that bone cells exhibit important biochemical responses upon the application of mechanical strain, such as the production of nitric oxide [13], collagen type I [39] and *c-fos* gene expression [40]. However, the mechanical strain required to elicit an osteogenic response from bone cells in vitro is much higher (~10,000με) [41, 42] than typical tissue level strains measured in vivo (~2,000με) [32]. This study found that for the osteocyte that received the maximum stimulus, there was a strain amplification factor of 9 when cellular level strains were compared to tissue level strains. It has already been proposed that osteocytic processes mediate the adaptive response of osteocytes due to the significant local strain amplifications in these regions [6, 16, 17, 26] and the fact that these regions have been shown to be more mechanosensitive than the cell body under micro-probing experiments [43]. The key findings of the current study indicate that the mechanical stimulus experienced by osteocytes within cortical bone tissue is highly dependent on local microstructural features. We report that the highest levels of strain occurred in the cell process of the osteocyte and that these

strains were further increased when the cellular submodel was directly adjacent to a Volkmann Canal, experiencing values much greater than 10,000με, which is higher than the threshold of mechanical strain required to elicit an osteogenic response from bone cells in vitro [41]. These results suggest that it is osteocytes located in the vicinity of micro-porosity, e.g. vascular canals, resorption cavities or micro-damage, that microstructural strain amplification effects are greatest and also that osteocytic cell processes in these locations may receive sufficient mechanical stimulation to elicit an osteogenic response. Also, these results indicate that the local lamellar orientation has a distinct effect on strain transfer into the cell, with greater stimuli being transferred to the cellular level when an orientation of +45°/-45° is considered. This finding has important implications as lamellar organisation in a particular osteon is thought to be dependent on local loading characteristics [44-46], with several different types of lamellar orientations observed experimentally using circularly polarized light (CPL) microscopy [44-46]. Furthermore, it has been observed that the local orientation of collagen fibres in perilacunar regions may differ from that of the surrounding osteon [47]. Although we do not consider such local variations in the osteon micro-environment, our results clearly highlight the important contribution that collagen fibre orientation has in determining the stimulus transferred to the cellular level.

Interestingly, these results also highlight that certain osteocytes in cortical bone receive very little mechanical stimulation due to their location within the microstructure. For the osteocyte that received the smallest stimulus, the majority of its volume experiences a strain of less than 2,000με, which is actually lower than applied tissue level strain. This osteocyte was also located directly adjacent to a Volkmann Canal however it was aligned with the direction of the applied load and was therefore subject to strain relieving effects at the microstructural level. It may be concluded that regions surrounding micro-pores represent the extremes of the stimulus being received by osteocytes in the cortical microstructure. In contrast, osteocytes that are not located near a micro-pore experience a more homogeneous microstructural strain field

and strain amplification factors in these cells are closer to average values. Furthermore, based on the findings of in vitro cell mechanobiology experiments [41, 42], a number of these cells do not receive sufficient stimulus (>10,000με) to initiate an adaptive response, whereas those in the vicinity of micro-pores are sufficiently stimulated. It is important to note that such experiments [41, 42], applied a homogeneous strain field to the entire cell using substrate stretching, whereas our model predicts that stimulation beyond 10,000με occurs only very localised regions along the cell processes. It is not clear whether such a localised stimulus would be sufficient to achieve an osteogenic response. Nonetheless, our findings show that a much greater proportion of osteocytes cells near micro-pores experience strain levels higher than this threshold, when compared to those exposed to a homogeneous microstructural strain field. Therefore, we propose that only a subset of osteocytes are involved in the mechanotransduction process in cortical bone tissue. Interestingly, evidence of primary cilia based mechanosensors have only been reported on 4% of osteocytes [48], which might support the hypothesis that the adaptive response of cortical bone tissue is possibly controlled by a certain subset of osteocytes. Furthermore, it has recently been shown by Guo et al [50] that stimulation of single osteocytes in vitro can lead calcium signalling responses throughout an osteocytic network. These data support the hypothesis that biochemical responses could be mediated by a small number of osteocytes that cause a cascade of responses throughout the entire osteocyte network. However further studies are required to quantify the distribution of mechanoreceptors on osteocytes to definitively address whether a subset of osteocytes act as mechanosensors in bone tissue.

It should be noted that osteocytes are also distributed throughout trabecular bone, which is not vascularised but still undergoes highly adaptive changes in response to mechanical loading. However, from finite element reconstructions of micro-CT data, it is known that the irregular micro-architecture of trabecular bone leads to an inhomogeneous strain field under loading [24, 25]. This would contribute to osteocytes in trabecular bone experiencing a wide range of

strains, depending on their location within the tissue and a similar progressive localisation framework that presented here could be used to characterise the local range of stimulus experienced by osteocytes in trabecular bone. Importantly, the findings of the current study highlight the importance of accounting for the structural hierarchy within bone tissue and the continued development of such multiscale techniques will enable a better understanding of the cellular mechanisms that mediate the in vivo adaptive response of the tissue.

5.0 Conclusions

In this study, we develop a novel multiscale finite element model that predicts how organ level loads are transmitted to osteocytes and their surrounding environment, by considering two levels of structural hierarchy within cortical bone tissue. It was found that an inhomogeneous microstructural strain field contributed to osteocytes receiving a vastly different stimulus at the cellular level, depending on their location within the microstructure. Furthermore, the principal orientation of lamellar regions was found to contribute significantly to the magnitude of the stimulus being received at the cellular level. Osteocytes that were in close proximity to a Volkmann Canal received the extremes of the stimulus in the cortical microstructure, due to both strain amplifications and relieving effects of the vascular cavity. In particular, osteocytes that directly adjacent to Volkmann Canals relative to the loading direction experienced strains that exceed the strain stimulus for osteogenesis (>10,000με) . In contrast, osteocytes not located near a micro-pore experience a homogeneous microstructural strain field and in many of these cells strains are lower and in some cases are insufficient to elicit an osteogenic response (<10,000με). Therefore, we propose that all osteocytes are not equal in terms of the mechanical stimulus being received and that only a subset of osteocytes that are located in close proximity to micro-pores may actually function as mechanoreceptors in cortical bone tissue.

Acknowledgements

This authors wish to acknowledge the funding provided by the European Research Council (ERC) under grant number 258992 (BONEMECHBIO).

References

[1] S.C. Cowin, L. Moss-Salentijn, and M.L. Moss: Candidates for the Mechanosensory System in Bone. *Journal of Biomechanical Engineering*, 113:2 (1991), 191-197.

[2] A.J. el Haj, S.L. Minter, S.C.F. Rawlinson, R. Suswillo, and L.E. Lanyon: Cellular responses to mechanical loading in vitro. *Journal of Bone and Mineral Research*, 5:9 (1990), 923-932.

[3] L.E. Lanyon: Functional strain as a determinant for bone remodeling. *Calcified Tissue International*, 36:1 (1984), S56-S61.

[4] J. Litzenberger, J.-B. Kim, P. Tummala, and C. Jacobs: β1 Integrins Mediate Mechanosensitive Signaling Pathways in Osteocytes. *Calcified Tissue International*, 86:4 (2010), 325-332.

[5] L.M. McNamara, R.J. Majeska, S. Weinbaum, V. Friedrich, and M.B. Schaffler: Attachment of Osteocyte Cell Processes to the Bone Matrix. *The Anatomical Record: Advances in Integrative Anatomy and Evolutionary Biology*, 292:3 (2009), 355-363.

[6] Y. Wang, L.M. McNamara, M.B. Schaffler, and S. Weinbaum: A model for the role of integrins in flow induced mechanotransduction in osteocytes. *Proceedings of The National Academy of Sciences*, 104:40 (2007), 15941-15946.

[7] A.I. Alford, C.R. Jacobs, and H.J. Donahue: Oscillating fluid flow regulates gap junction communication in osteocytic MLO-Y4 cells by an ERK1/2 MAP kinase-dependent mechanism☆. *Bone*, 33:1 (2003), 64-70.

[8] B. Cheng, S. Zhao, J. Luo, E. Sprague, L.F. Bonewald, and J.X. Jiang: Expression of Functional Gap Junctions and Regulation by Fluid Flow in Osteocyte-Like MLO-Y4 Cells. *Journal of Bone and Mineral Research*, 16:2 (2001), 249-259.

[9] D.A. Hoey, J.C. Chen, and C.R. Jacobs: The Primary Cilium as a Novel Extracellular Sensor in Bone. *Frontiers in Endocrinology*, 3:(2012).

[10] D.A. Hoey, D.J. Kelly, and C.R. Jacobs: A role for the primary cilium in paracrine signaling between mechanically stimulated osteocytes and mesenchymal stem cells. *Biochemical and Biophysical Research Communications*, 412:1 (2011), 182-187.

[11] A.M.D. Malone, C.T. Anderson, P. Tummala, R.Y. Kwon, T.R. Johnston, T. Stearns, and C.R. Jacobs: Primary cilia mediate mechanosensing in bone cells by a calcium-independent mechanism. *Proceedings of the National Academy of Sciences, USA*, 104:33 (2007), 13325-13330.

[12] R.L. Duncan and C.H. Turner: Mechanotransduction and the functional response of bone to mechanical strain. *Calcified Tissue International*, 57:5 (1995), 344-358.

[13] M. Mullender, A.J. Haj, Y. Yang, M.A. Duin, E.H. Burger, and J. Klein-Nulend: Mechanotransduction of bone cellsin vitro: Mechanobiology of bone tissue. *Medical and Biological Engineering and Computing*, 42:1 (2004), 14-21.

[14] D. Nicolella, L. Bonewald, D. Moravits, and J. Lankford: Measurement of microstructural strain in cortical bone. *European Journal of Morphology*, 42:1-2 (2005), 23-29.

[15] D.P. Nicolella, D.E. Moravits, A.M. Gale, L.F. Bonewald, and J. Lankford: Osteocyte lacunae tissue strain in cortical bone. *Journal of Biomechanics*, 39:9 (2006), 1735-1743.

[16] S.W. Verbruggen, T.J. Vaughan, and L.M. McNamara: Strain amplification in bone mechanobiology: a computational investigation of the in vivo mechanics of osteocytes. *J R Soc Interface*, 9:75 (2012), 2735-44.

[17] A. Rath Bonivtch, L.F. Bonewald, and D.P. Nicolella: Tissue strain amplification at the osteocyte lacuna: A microstructural finite element analysis. *Journal of Biomechanics*, 40:10 (2007), 2199-2206.

[18] S. Weinbaum, S.C. Cowin, and Y. Zeng: A model for the excitation of osteocytes by mechanical loading-induced bone fluid shear stresses. *Journal of Biomechanics*, 27:3 (1994), 339-360.

[19] E. Anderson, S. Kaliyamoorthy, J. Alexander, and M. Tate: Nano–Microscale Models of Periosteocytic Flow Show Differences in Stresses Imparted to Cell Body and Processes. *Annals of Biomedical Engineering*, 33:1 (2005), 52-62.

[20] Y. Han, S.C. Cowin, M.B. Schaffler, and S. Weinbaum: Mechanotransduction and strain amplification in osteocyte cell processes. *Proceedings of the National Academy of Sciences of the United States of America*, 101:47 (2004), 16689-16694.

[21] E.H. BURGER and J. KLEIN-NULEND: Mechanotransduction in bone□role of the lacuno-canalicular network. *The FASEB Journal*, 13:9001 (1999), 101-112.

[22] E.J. Anderson and M.L. Knothe Tate: Idealization of pericellular fluid space geometry and dimension results in a profound underprediction of nano-microscale stresses imparted by fluid drag on osteocytes. *Journal of Biomechanics*, 41:8 (2008), 1736-1746.

[23] L. You, S.C. Cowin, M.B. Schaffler, and S. Weinbaum: A model for strain amplification in the actin cytoskeleton of osteocytes due to fluid drag on pericellular matrix. *Journal of Biomechanics*, 34:11 (2001), 1375-1386.

[24] D. Ulrich, B. van Rietbergen, H. Weinans, and P. Rüegsegger: Finite element analysis of trabecular bone structure: a comparison of image-based meshing techniques. *Journal of Biomechanics*, 31:12 (1998), 1187-1192.

[25] N. Vilayphiou, S. Boutroy, E. Sornay-rendu, B. Van rietbergen, F. Munoz, P.D. Delmas, and R. Chapurlat: Finite element analysis performed on radius and tibia HR-pQCT images and fragility fractures at all sites in postmenopausal women. *Bone*, 46:4 (2010), 1030-1037.

[26] Y. Han: Mechanotransduction and strain amplification in osteocyte cell processes. *Proceedings of The National Academy of Sciences*, 101:47 (2004), 16689-16694.

[27] X.N. Dong and X.E. Guo: Geometric Determinants to Cement Line Debonding and Osteonal Lamellae Failure in Osteon Pushout Tests. *Journal of Biomechanical Engineering*, 126:3 (2004), 387-390.

[28] L.P. Mullins, J.P. McGarry, M.S. Bruzzi, and P.E. McHugh: Micromechanical modelling of cortical bone. *Computer Methods in Biomechanics and Biomedical Engineering*, 10:3 (2007), 159-169.

[29] T.J. Vaughan, C.T. McCarthy, and L.M. McNamara: A three-scale finite element investigation into the effects of tissue mineralisation and lamellar organisation in human cortical and trabecular bone. *Journal of the Mechanical Behavior of Biomedical Materials*, 12:0 (2012), 50-62.

[30] L.-D. You, S. Weinbaum, S.C. Cowin, and M.B. Schaffler: Ultrastructure of the osteocyte process and its pericellular matrix. *The Anatomical Record Part A: Discoveries in Molecular, Cellular, and Evolutionary Biology*, 278A:2 (2004), 505-513.

[31] L. Wang, Y. Wang, Y. Han, S.C. Henderson, R.J. Majeska, S. Weinbaum, and M.B. Schaffler: In situ measurement of solute transport in the bone lacunar-canalicular system. *Proceedings of*

the National Academy of Sciences of the United States of America, 102:33 (2005), 11911-11916.

[32] D.B. Burr, et al.: In vivo measurement of human tibial strains during vigorous activity. *Bone*, 18:5 (1996), 405-410.

[33] Y. Sugawara, et al.: The alteration of a mechanical property of bone cells during the process of changing from osteoblasts to osteocytes. *Bone*, 43:1 (2008), 19-24.

[34] L.G. Alexopoulos, M.A. Haider, T.P. Vail, and F. Guilak: Alterations in the Mechanical Properties of the Human Chondrocyte Pericellular Matrix With Osteoarthritis. *Journal of Biomechanical Engineering*, 125:3 (2003), 323-333.

[35] Y. Carter, C.D.L. Thomas, J.G. Clement, A.G. Peele, K. Hannah, and D.M.L. Cooper: Variation in osteocyte lacunar morphology and density in the human femur — a synchrotron radiation micro-CT study. *Bone*, 52:1 (2013), 126-132.

[36] J. Kaiser, T. Lemaire, S. Naili, V. Sansalone, and S.V. Komarova: Do calcium fluxes within cortical bone affect osteocyte mechanosensitivity? *J Theor Biol*, 303:0 (2012), 75-86.

[37] V. Sansalone, J. Kaiser, S. Naili, and T. Lemaire: Interstitial fluid flow within bone canaliculi and electro-chemo-mechanical features of the canalicular milieu. *Biomechanics and Modeling in Mechanobiology*, (2012), 1-21.

[38] T.H. Smit and E.H. Burger: Is BMU-Coupling a Strain-Regulated Phenomenon? A Finite Element Analysis. *Journal of Bone and Mineral Research*, 15:2 (2000), 301-307.

[39] D.B. Jones, H. Nolte, J.G. Scholübbers, E. Turner, and D. Veltel: Biochemical signal transduction of mechanical strain in osteoblast-like cells. *Biomaterials*, 12:2 (1991), 101-110.

[40] M.A. Peake, L.M. Cooling, J.L. Magnay, P.B.M. Thomas, and A.J. El Haj: Selected Contribution: Regulatory pathways involved in mechanical induction of c-fos gene expression in bone cells. *Journal of Applied Physiology*, 89:6 (2000), 2498-2507.

[41] J. You, C.E. Yellowley, H.J. Donahue, Y. Zhang, Q. Chen, and C.R. Jacobs: Substrate Deformation Levels Associated With Routine Physical Activity Are Less Stimulatory to Bone Cells Relative to Loading-Induced Oscillatory Fluid Flow. *Journal of Biomechanical Engineering, Transactions of the ASME*, 122:4 (2000), 387-393.

[42] E.H. Burger and J.P. Veldhuijzen: Influence of mechanical factors on bone formation, resorption, and growth in vitro. . *Hall, B. K. eds. Bone* 7:(1993), Vol. 7,37-56 CRC Press Boca Raton, FL.

[43] T. Adachi, Y. Aonuma, M. Tanaka, M. Hojo, T. Takano-Yamamoto, and H. Kamioka: Calcium response in single osteocytes to locally applied mechanical stimulus: Differences in cell process and cell body. *Journal of Biomechanics*, 42:12 (2009), 1989-1995.

[44] T.G. Bromage, H.M. Goldman, S.C. McFarlin, J. Warshaw, A. Boyde, and C.M. Riggs: Circularly polarized light standards for investigations of collagen fiber orientation in bone. *The Anatomical Record Part B: The New Anatomist*, 274B:1 (2003), 157-168.

[45] J.G. Skedros, M.W. Mason, M.C. Nelson, and R.D. Bloebaum: Evidence of structural and material adaptation to specific strain features in cortical bone. *The Anatomical Record*, 246:1 (1996), 47-63.

[46] H.M. Goldman, T.G. Bromage, C.D.L. Thomas, and J.G. Clement: Preferred collagen fiber orientation in the human mid-shaft femur. *The Anatomical Record Part A: Discoveries in Molecular, Cellular, and Evolutionary Biology*, 272A:1 (2003), 434-445.

[47] M.-G. Ascenzi, J. Gill, and A. Lomovtsev: Orientation of collagen at the osteocyte lacunae in human secondary osteons. *Journal of Biomechanics*, 41:16 (2008), 3426-3435.

[48] E.A. Tonna and N.M. Lampen: Electron microscopy of aging skeletal cells. I. Centrioles and solitary cilia. *J Gerontol*, 27:3 (1972), 316-24.

Figure Captions

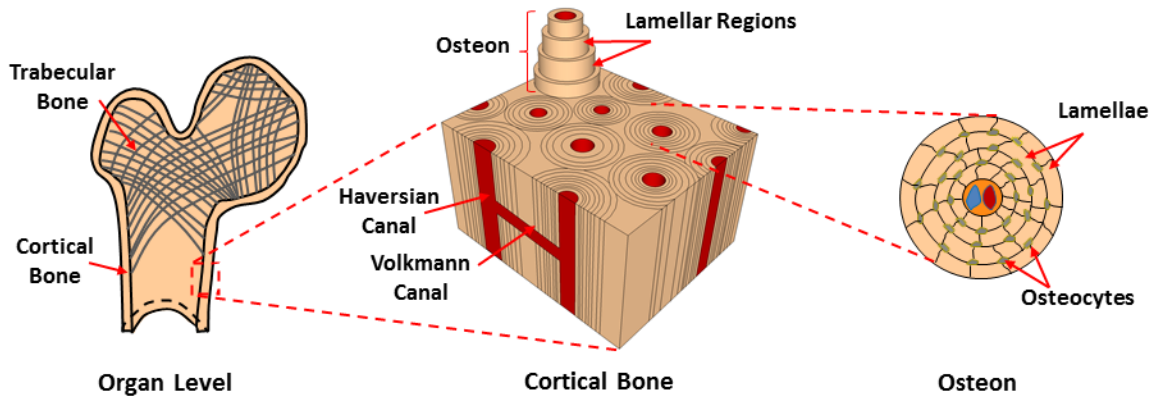

Figure 1: Hierarchical nature of bone tissue that depicts the inhomogeneous structure of cortical bone due to presence of Haversian and Volkmann Canals, discrete lamellar regions and osteocytes embedded within lacunar cavities.

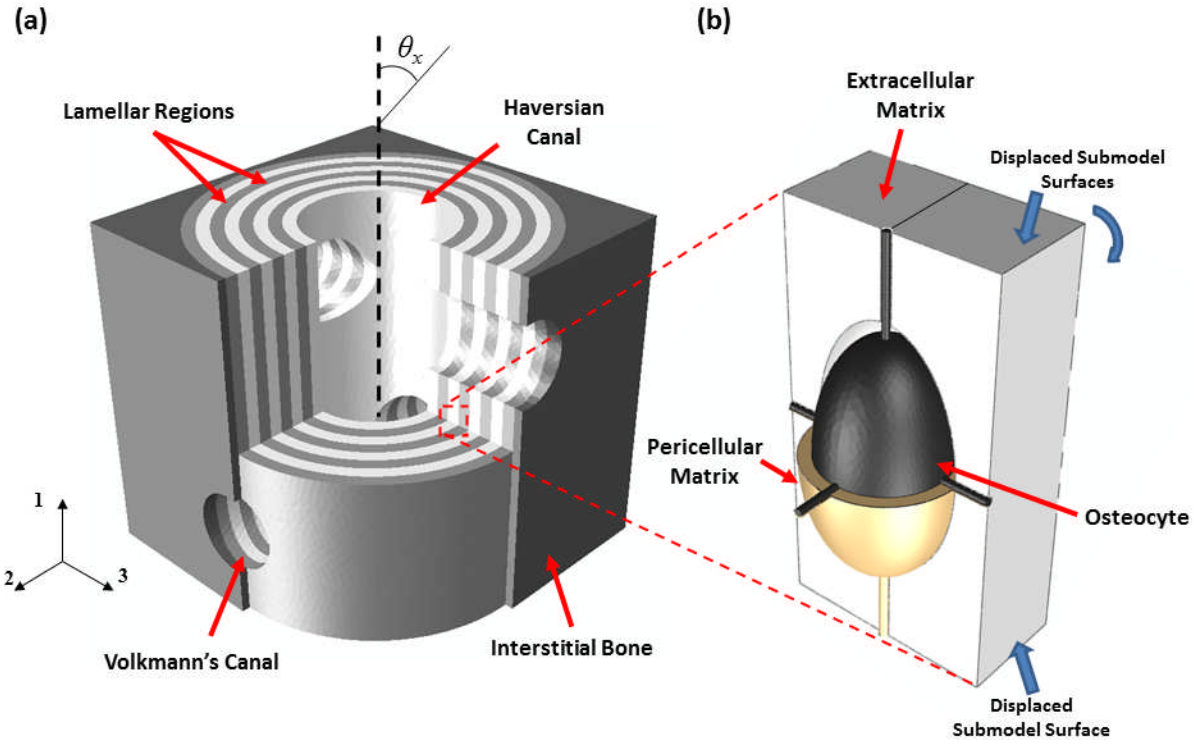

Figure 2: (a) Micromechanical model of cortical bone (sectioned view) and (b) Cellular level model of the osteocyte environment (sectioned view).

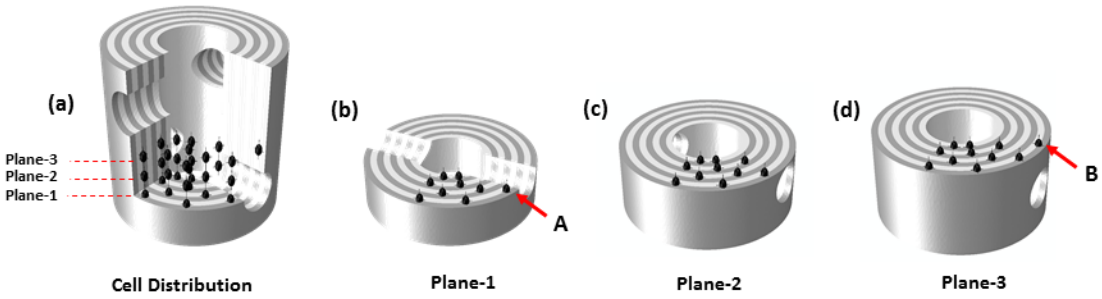

Figure 3: (a) Distribution of cellular submodels that are analysed on (b) Plane-1 (c) Plane-2 and (d) Plane-3.

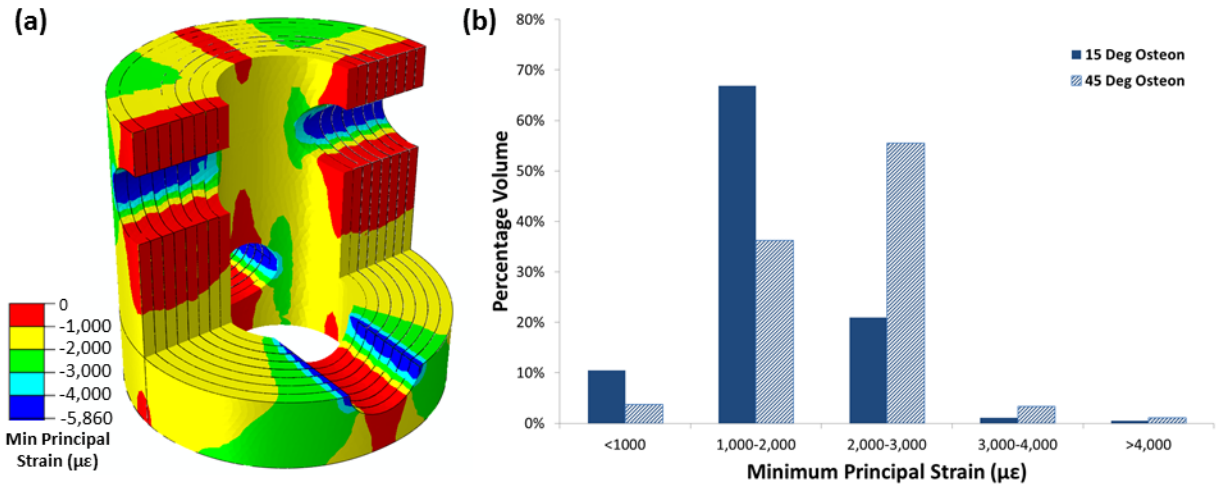

Figure 4: (a) Distribution of Minimum Principal Strain in a sectioned view of the osteon model under a compressive load of -2,000με and (b) Volume average distribution of Minimum Principal Strain in the Osteon Model under a compressive load of -2,000με.

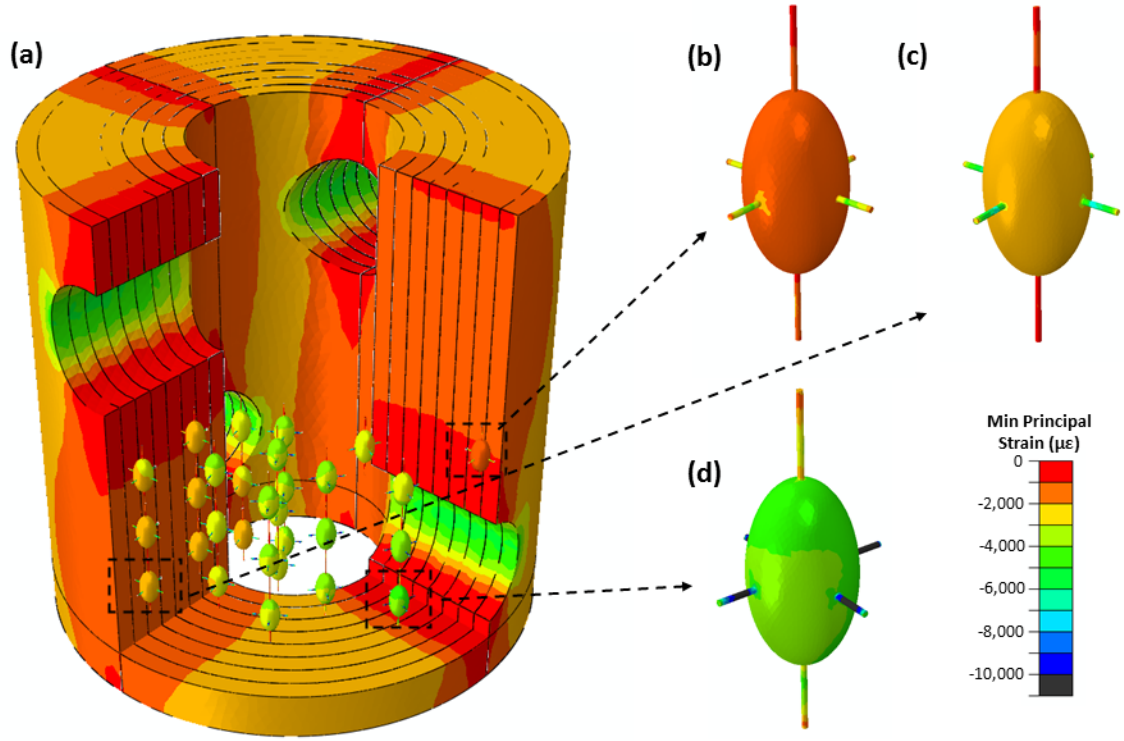

Figure 5: Distribution of minimum principal strain in a number of different osteocytes located in different regions of the osteon.

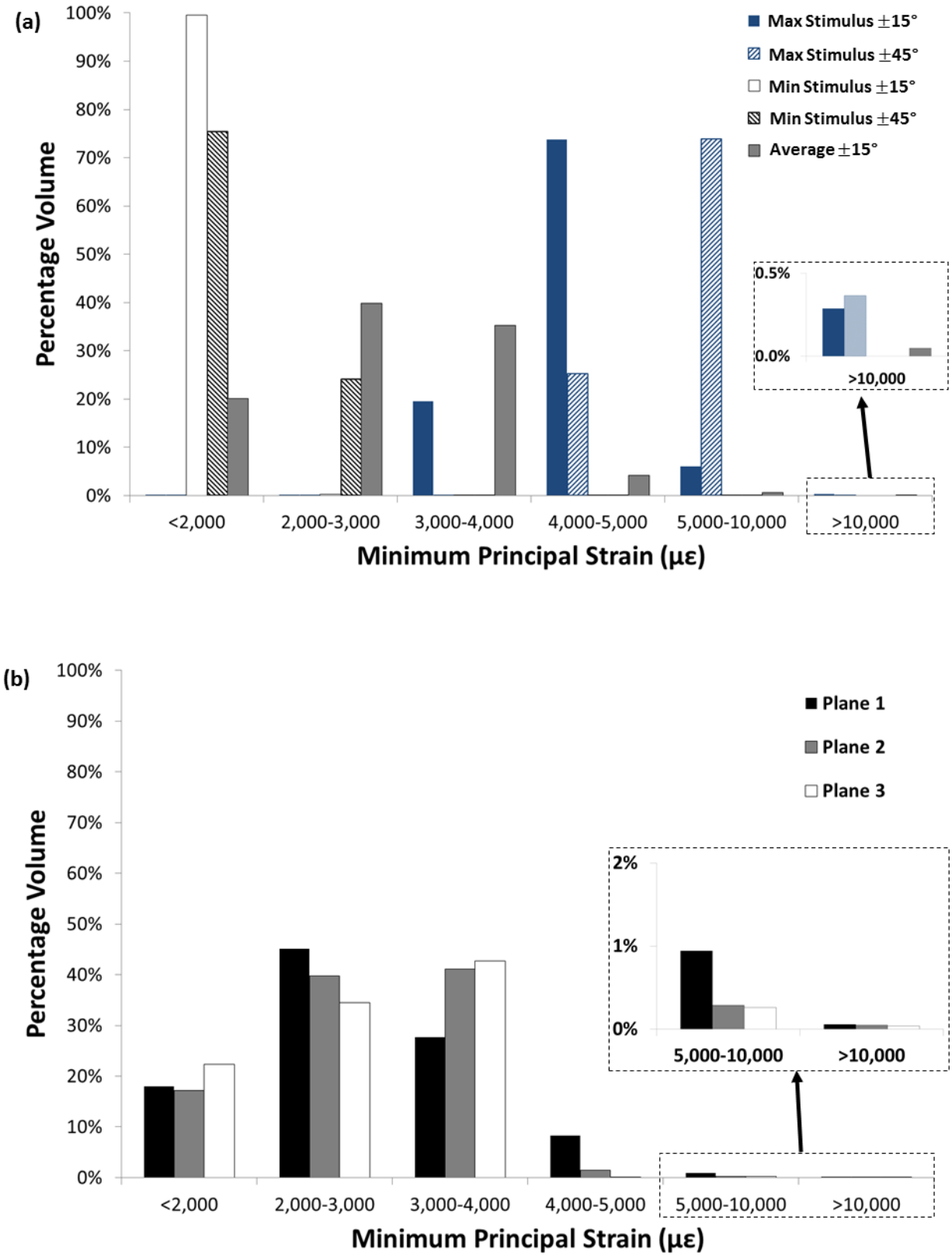

Figure 6: Volume average distribution of minimum principal strain at the cellular level for (a) a range of different osteocytes and (b) average values of osteocytes from each Plane considered for +15°/-15° lamellar orientation.

Tables

Table 1: Material parameters for lamellar bone

E_x	E_y	E_z	G_{xy}	G_{yz}	G_{xz}
18.71 GPa	3.2 GPa	9.696 GPa	0.824 GPa	0.824 GPa	4.05 GPa
υ_{xy}	υ_{yz}	υ_{zx}	υ_{yx}	υ_{zy}	υ_{xz}
0.352	0.13	0.0823	0.0604	0.3965	0.1605